



Sample thickness dependence of giant magnetoimpedance under low fields for $\text{La}_{0.67}\text{Sr}_{0.33}\text{Mn}_{0.98}\text{Co}_{0.02}\text{O}_3$ manganites

Jifan Hu^{a,*}, Yifei Wang^a, Yongjia Zhang^a, Hua Liu^a, Hongwei Qin^a, Bo Li^b

^a Department of Physics, State Key Laboratory for Crystal Materials, Shandong University, Jinan 250100, China

^b Department of Functional Materials, Central Iron and Steel Research Institute, Beijing 100081, China

ARTICLE INFO

Article history:

Received 16 July 2010

Received in revised form 17 October 2010

Accepted 21 October 2010

Available online 29 October 2010

PACS:

75.47. Lx

Keywords:

Manganites

Magnetoimpedance

ABSTRACT

The $\text{La}_{0.67}\text{Sr}_{0.33}\text{Mn}_{0.98}\text{Co}_{0.02}\text{O}_3$ plate sintered at 1250 °C shows a low field magnetoresistance (LFMR) effect under fields $H < 4.6$ kOe. However, the DC magnetoresistance $\Delta R/R_0$ is very small, only -1.84% under $H = 4.6$ kOe. The character of helical growth was observed on grain surface of $\text{La}_{0.67}\text{Sr}_{0.33}\text{Mn}_{0.98}\text{Co}_{0.02}\text{O}_3$ phase. The LFMR is connected with the interface of grain or grain boundary, while the giant magnetoimpedance under low fields for $\text{La}_{0.67}\text{Sr}_{0.33}\text{Mn}_{0.98}\text{Co}_{0.02}\text{O}_3$ sintered plates strongly depends upon the plate thickness. With an increase of sample thickness, the magnetoimpedance increases and the frequency, where the maximum magnetoimpedance occurs, shifts to low frequencies. A giant magnetoimpedance of -15.6% and a large AC magnetoresistance of -30.5% could be obtained under a very small field $H = 600$ Oe for the plate with a thickness of 3 mm.

© 2010 Elsevier B.V. All rights reserved.

1. Introduction

Perovskite manganites $\text{La}_{1-x}\text{A}_x\text{MnO}_3$ ($A = \text{Ca}, \text{Ba}, \text{Sr}$ and Pb) have attracted great attention due to the colossal magnetoresistance (CMR) [1,2]. The colossal magnetoresistance (CMR) could be explained in term of the double-exchange interaction [3] and electron–phonon coupling [4]. One of the problems limited practical applications of the CMR is the small value of magnetoresistance $\Delta R/R_0$ at room temperature under a low magnetic field. Hence, many investigations focus on the low-field magnetoresistance (LFMR) in polycrystalline manganites. The spin-polarized tunneling through the interfaces of grains or spin-dependent scattering at grain boundaries has been suggested to be responsible for the LFMR [5,6]. In addition to CMR and LFMR, $\text{La}_{1-x}\text{A}_x\text{MnO}_3$ based manganites also exhibit colossal magnetoabsorption in the microwave high-frequencies ($\sim \text{GHz}$) [7,8] and giant magnetoimpedance in radio frequencies ($\sim \text{MHz}$) [9–24]. For metallic manganites below Curie temperature, a high frequency current passes the sample mainly through its surface region characterized by the penetration depth $\delta = \sqrt{2\rho/\mu_0\mu_t\omega}$ (ρ is the resistivity, μ_0 vacuum permeability, μ_t transverse permeability of material, ω the angular frequency of current) and a strong magnetoimpedance could occur, which originates from the variation of μ_t induced by the applied DC magnetic field, via the change of penetration depth δ . The giant

magnetoimpedance effect has also been found in soft magnetic ribbons and wires [25–28]. The conductivity mechanism for manganites is completely different from those of conventional soft magnetic ribbons and wires. In addition, there is a strong interplay among lattice, electronic transport and magnetic properties in manganites. Compared with extensive studies on the CMR/LFMR for manganites and the giant magnetoimpedance (GMI) for the soft magnetic ribbons and wires, up to now, few investigations on magnetoimpedance for manganites were done. According to the classical electrodynamics, the value of parameter d/δ (where d is the half of the sample thickness) characterizes the magnitude of skin effect [29]. To our knowledge, there is no research report on the sample thickness dependence of magnetoimpedance for manganites yet. In the present work, we observed the LFMR for $\text{La}_{0.67}\text{Sr}_{0.33}\text{Mn}_{0.98}\text{Co}_{0.02}\text{O}_3$ plate sintered at relative lower temperature (1250 °C). The character of helical growth was observed on grain surface of $\text{La}_{0.67}\text{Sr}_{0.33}\text{Mn}_{0.98}\text{Co}_{0.02}\text{O}_3$ phase. We found that the skin effect still depends strongly upon the thickness of manganite sample, where LFMR effect occurs at the DC case. Larger magnetoimpedance could be found for the thicker manganite sample at a lower frequency. The $\text{La}_{0.67}\text{Sr}_{0.33}\text{Mn}_{0.98}\text{Co}_{0.02}\text{O}_3$ plate with a thickness of 3 mm exhibits a magnetoimpedance $\Delta Z/Z_0$ of -15.6% at 3 MHz under a very low field $H = 600$ Oe, whereas its DC magnetoresistance $\Delta R/R_0$ is very small, only -1.84% under $H = 4.6$ kOe.

2. Experimental

The $\text{La}_{0.67}\text{Sr}_{0.33}\text{Mn}_{0.98}\text{Co}_{0.02}\text{O}_3$ plate was prepared by the conventional solid state reaction with a sintering temperature of 1250 °C for 24 h. The room-temperature

* Corresponding author. Tel.: +86 531 88566143; fax: +86 531 88377031.
E-mail address: hu-jf@vip.163.com (J. Hu).

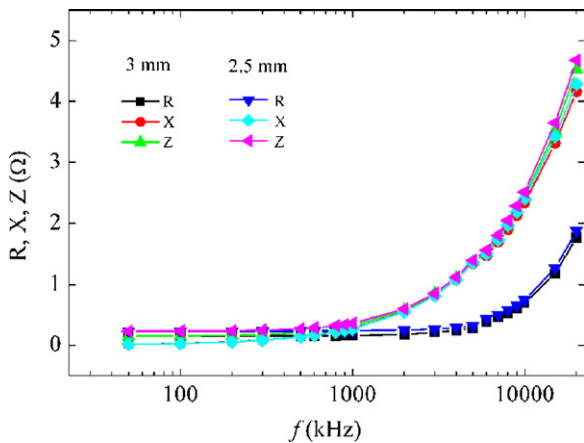


Fig. 1. The AC frequency dependence of impedance, resistance as well as reactance for $\text{La}_{0.67}\text{Sr}_{0.33}\text{Mn}_{0.98}\text{Co}_{0.02}\text{O}_3$ sintered plates with $D = 2.5$ and 3 mm.

resistivity ρ was measured as about $0.017 \Omega\text{cm}$ by a four terminal method. The DC magnetoresistance for $\text{La}_{0.67}\text{Sr}_{0.33}\text{Mn}_{0.98}\text{Co}_{0.02}\text{O}_3$ sintered plate was measured at room temperature. The impedance behavior at room temperature for $\text{La}_{0.67}\text{Sr}_{0.33}\text{Mn}_{0.98}\text{Co}_{0.02}\text{O}_3$ sintered plate (with 22 mm length and 5 mm width) was measured using an impedance analyzer (HP4294A), where the amplitude of the AC current was 20 mA. Four Au electrodes were evaporated on one surface of the plate. The distance of voltage terminals on the sample was 15 mm. The sample was connected to the analyzer with the accessory test lead, which is carefully designed and contains four coaxial cables. The sample thickness D was adjusted from 3 to 1.5 mm by polishing the surface opposite to the surface containing four electrodes. The longitudinal magnetoimpedance measurement was performed, where both AC currents and DC magnetic fields were applied along the sample length.

3. Results and discussion

The Curie temperature was 354 K and metal-insulator transition temperature was 342 K for $\text{La}_{0.67}\text{Sr}_{0.33}\text{Mn}_{0.98}\text{Co}_{0.02}\text{O}_3$, which behaved as a metal at the room temperature. The AC frequency dependence of impedance, resistance as well as reactance for $\text{La}_{0.67}\text{Sr}_{0.33}\text{Mn}_{0.98}\text{Co}_{0.02}\text{O}_3$ sintered plate with $D = 2.5$ and 3 mm are shown in Fig. 1. The skin effect can be clearly observed at high frequencies. The frequency with $X/R = 1$ locates at 543 kHz for $D = 3$ mm, and 861 kHz for $D = 2.5$ mm. According to the classical electrodynamics [29], the complex impedance $Z = R + iX$ of metallic flake with thickness $D = 2d$, when an AC current flows through the flake along the length direction, can be obtained as [30]

$$Z = R_{DC}kd \coth(kd) \quad (1)$$

with $k = (1 + i)/\delta$. It can be derived from Eq. (1) that $R = X$ holds when $d/\delta = 1.57$, and $d/\delta = 1$ corresponds to $X/R \approx 0.59$. The frequency with $X/R \approx 0.59$ locates at 324 kHz for $D = 3$ mm, and 499 kHz for $D = 2.5$ mm. The strength of skin effect is stronger for the thicker than for the thinner. The observed results on skin effect for $\text{La}_{0.67}\text{Sr}_{0.33}\text{Mn}_{0.98}\text{Co}_{0.02}\text{O}_3$ sintered plate are consistent with the principle of classical electrodynamics.

The DC field dependence of room temperature magnetoresistance $\Delta R/R_0$ for $\text{La}_{0.67}\text{Sr}_{0.33}\text{Mn}_{0.98}\text{Co}_{0.02}\text{O}_3$ plate sintered at 1250°C is shown in Fig. 2. The $\text{La}_{0.67}\text{Sr}_{0.33}\text{Mn}_{0.98}\text{Co}_{0.02}\text{O}_3$ sintered plate shows a sharp drop in R under low fields $H < 4.6$ kOe, followed by a slow decrease in R under high fields. The DC magnetoresistance $\Delta R/R_0$ is very small, only -1.84% under $H = 4.6$ kOe. The microstructure of $\text{La}_{0.67}\text{Sr}_{0.33}\text{Mn}_{0.98}\text{Co}_{0.02}\text{O}_3$ plate is observed by a field emission scanning microscopy (FESEM), and typical image is shown in Fig. 3. No rich-Co impurity phases could be found by the observation with FESEM and energy dispersive spectroscopy (EDS). The character of helical growth is evident on grain surface (see Fig. 3). The low field magnetoresistance (LFMR) is usually attributed to spin-polarized tunneling through the magnetically disordered

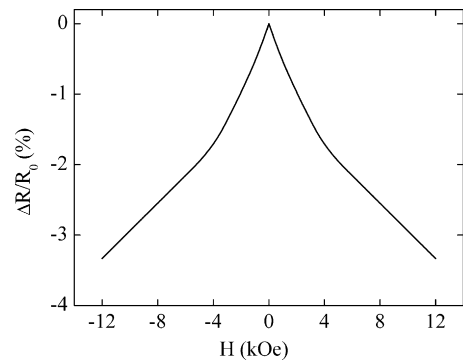


Fig. 2. The DC field dependence of magnetoresistance for $\text{La}_{0.67}\text{Sr}_{0.33}\text{Mn}_{0.98}\text{Co}_{0.02}\text{O}_3$ plate at room temperature.

interface barriers or spin dependent scattering at the grain boundaries. For high temperature sintering (1300°C), the LFMR effect is hardly observed for $\text{La}_{0.67}\text{Sr}_{0.33}\text{Mn}_{0.98}\text{Co}_{0.02}\text{O}_3$ plate [31]. The LFMR of $\text{La}_{2/3}\text{Sr}_{1/3}\text{MnO}_3$ is evident at low temperatures, and becomes more negligible at room temperature with an increase of annealing temperature from 1300 to 1700°C [5].

As shown in Fig. 4, for $\text{La}_{0.67}\text{Sr}_{0.33}\text{Mn}_{0.98}\text{Co}_{0.02}\text{O}_3$ manganite with $D = 3$ mm under a very low field $H = 600$ Oe, the magnetoimpedance $\Delta Z/Z_0 = (Z(H) - Z(0))/Z(0)$ is -15.6% at 3 MHz, and AC magnetoresistance $\Delta R/R_0 = (R(H) - R(0))/R(0)$ reaches -30.5% at 7 MHz, more sensitive than the DC magnetoresistance ($\Delta R/R_0 = -1.84\%$ under $H = 4.6$ kOe). The magnetoimpedance depends sensitively upon frequency f of AC current, DC magnetic field H and sample thickness $D = 2d$. The frequency dependence of magnetoimpedance $\Delta Z/Z_0$, magnetoresistance $\Delta R/R_0$ and magnetoreactance $\Delta X/X_0$ under $H = 600$ Oe for $\text{La}_{0.67}\text{Sr}_{0.33}\text{Mn}_{0.98}\text{Co}_{0.02}\text{O}_3$ plates (with $D = 1.5$, 2.5 and 3 mm) at room temperature are shown in Fig. 5. For low frequencies ($d/\delta \ll 1$) where skin effect is very weak, the expressions of $R = R_{DC}[1 + \frac{4}{45}(d/\delta)^4] \approx R_{DC}$ and $X = \frac{2}{3}R_{DC}(d/\delta)^2$ hold [30]. A strong magnetoreactance effect can be observed at low frequencies, where $\Delta X/X_0$ is proportional to $\Delta\mu_t/\mu_t(0)$ [32]. The magnetoresistance is very small, since the skin effect is very weak when $d/\delta \ll 1$. As the X value is much smaller than R value, the magnetoimpedance is negligible. With an increase of frequency, the skin effect becomes pronounced. At very high frequencies, the impedance sensitively depends on the penetration depth δ and is proportional to the term of $\sqrt{\mu_0\mu_t\omega\rho}$ [19], the applied magnetic field could induce not only the reduction of the resistivity ρ but also a decrease of transverse permeability μ_t , leading to a drop of impedance Z . It can be seen from Fig. 2

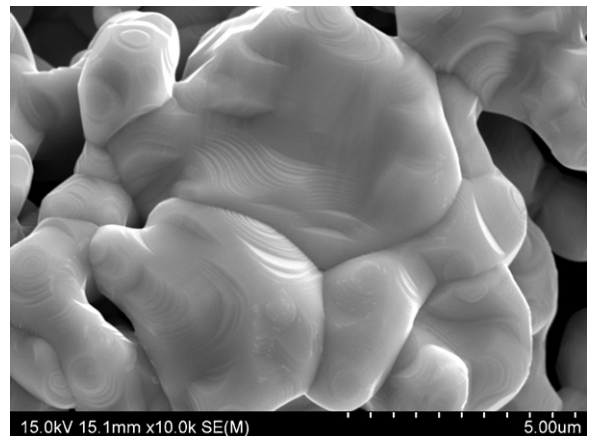


Fig. 3. The typical microstructure for $\text{La}_{0.67}\text{Sr}_{0.33}\text{Mn}_{0.98}\text{Co}_{0.02}\text{O}_3$ plate.

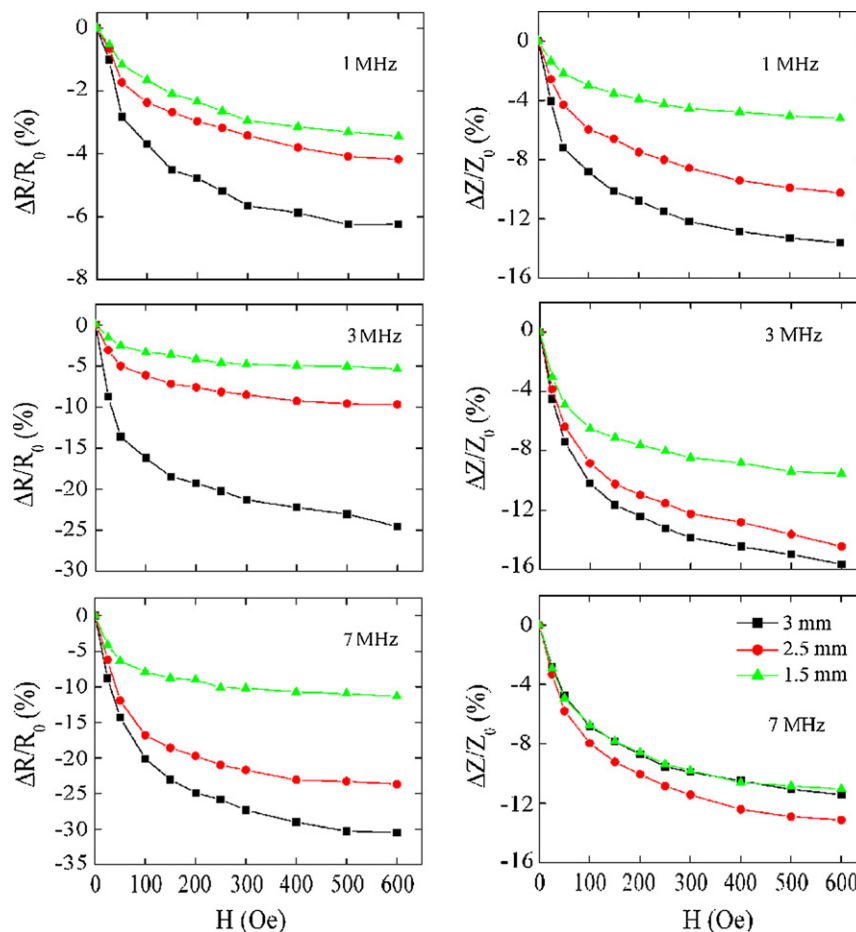


Fig. 4. The DC field dependence of AC magnetoresistance $\Delta R/R_0$ and magnetoimpedance $\Delta Z/Z_0$ for $\text{La}_{0.67}\text{Sr}_{0.33}\text{Mn}_{0.98}\text{Co}_{0.02}\text{O}_3$ manganites with $D = 1.5, 2.5$ and 3 mm.

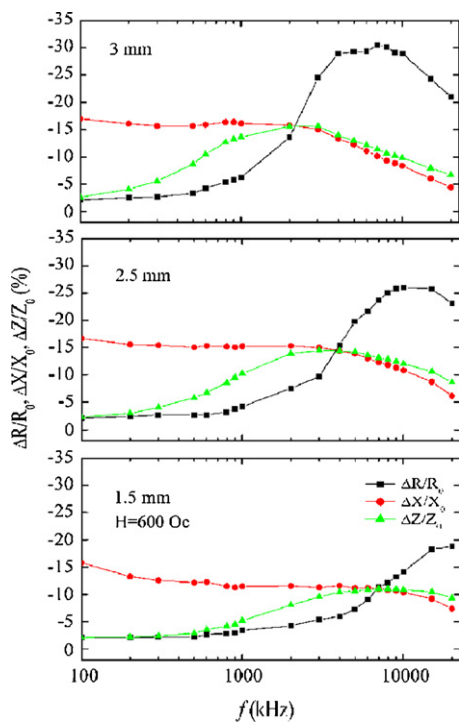


Fig. 5. The frequency dependence of magnetoimpedance $\Delta Z/Z_0$, magnetoresistance $\Delta R/R_0$ and magnetoreactance $\Delta X/X_0$ under $H = 600$ Oe for $\text{La}_{0.67}\text{Sr}_{0.33}\text{Mn}_{0.98}\text{Co}_{0.02}\text{O}_3$ plates with $D = 1.5, 2.5$ and 3 mm.

that at room temperature the change of dc resistivity $\Delta\rho/\rho_0$ (or DC magnetoresistance $\Delta R/R_0$) is very small under low fields and its contribution to the change of impedance Z is little. The magnetoimpedance $\Delta Z/Z_0$ is mainly due to the permeability change. As shown in Fig. 5, the magnetoimpedance $\Delta Z/Z_0$ increases at first, undergoes its maximum $(\Delta Z/Z_0)_{\max}$ at a certain frequency f (MI_{\max}), and finally drops again. The magnetoresistance $\Delta R/R_0$ also experiences a peak $(\Delta R/R_0)_{\max}$ at a frequency f (MR_{\max}), whereas the magnetoreactance $\Delta X/X_0$ almost decreases with increasing AC current frequencies. It should be noted that the values of magnetoresistance $\Delta R/R_0$ and magnetoimpedance $\Delta Z/Z_0$ at 100 kHz remain almost the same for all three pellets with different thickness of $D = 1.5, 2.5$ and 3 mm, when an ac current of 20 mA is used (see Fig. 5). The value of $(\Delta Z/Z_0)_{\max}$ under $H = 600$ Oe for $\text{La}_{0.67}\text{Sr}_{0.33}\text{Mn}_{0.98}\text{Co}_{0.02}\text{O}_3$ plates is -15.6% for $D = 3$ mm, -14.5% for $D = 2.5$ mm and -11% for $D = 1.5$ mm. The corresponding frequency f (MI_{\max}) shifts from 3 MHz for $D = 3$ mm to 7 MHz for $D = 1.5$ mm. The thicker sample has a lower frequency f (MI_{\max}) than the thinner, since the former has a stronger skin effect than the later. Recently, similar sample thickness dependence of giant magnetoimpedance was also observed in sol-gel nanocrystalline manganites [33].

The frequency f (MI_{\max}) dependence on the sample thickness D could be estimated using Eq. (1) with $\mu_t = 30$, $\Delta\mu_t/\mu_t(0) = -20\%$ and $\rho = 0.017 \Omega \text{ cm}$, neglecting the effect of domain wall relaxation for a crude approximation. The calculated value of the frequency f (MI_{\max}) is $7.84, 4.35, 2.87$ and 1.96 MHz for $D = 1.5, 2, 2.5$ and 3 mm, respectively. Usually, the domain wall relaxation in soft magnetic materials brings about the drop of permeability change $\Delta\mu_t/\mu_t(0)$ with an increase of frequency f . The drop of $(\Delta Z/Z_0)_{\max}$ with a

decrease of sample thickness could be attributed to the decrease of permeability change $\Delta\mu_t/\mu_t(0)$ at a higher frequency f (M_{max}).

The giant magnetoimpedance is associated with the field-induced change of transverse permeability via the penetration depth. The field induced change of permeability depends upon not only the electric and magnetic properties of manganite phase, but also the microstructure of sample since the movement of magnetic domain could be influenced by the defects or grain boundaries through the pinning effect. Thus, the magnitude of magnetoimpedance for a manganite is also connected with both properties of manganite phase and microstructure of sample.

4. Conclusions

The $\text{La}_{0.67}\text{Sr}_{0.33}\text{Mn}_{0.98}\text{Co}_{0.02}\text{O}_3$ plate sintered at 1250°C shows a low field magnetoresistance effect under fields $H < 4.6\text{ kOe}$. However the DC magnetoresistance $\Delta R/R_0$ is very small, only -1.84% under $H = 4.6\text{ kOe}$. The character of helical growth was observed on grain surface of $\text{La}_{0.67}\text{Sr}_{0.33}\text{Mn}_{0.98}\text{Co}_{0.02}\text{O}_3$ phase. The low field magnetoresistance (LFMR) could be attributed to spin-polarized tunneling through interface barriers of grains or spin dependent scattering at the grain boundaries. A giant magnetoimpedance of -15.6% and a large AC magnetoresistance of -30.5% could be obtained under a very small field $H = 600\text{ Oe}$ for the plate with a thickness of 3 mm . Larger magnetoimpedance could be found for the thicker sample at a lower frequency. The magnetoimpedance effect of manganites provides an alternative route for possible application in magnetic recording and sensing.

Acknowledgement

This work was supported by National Natural Science Foundation of China (Grant Nos: 50872074, 50872069 and 51072103).

References

- [1] R. von Helmolt, J. Wecker, B. Holzapfel, L. Schultz, K. Samwer, Phys. Rev. Lett. 71 (1993) 2331.
- [2] S. Jin, T.H. Tiefel, M. McCormack, R.A. Fastnacht, R. Ramesh, L.H. Chen, Science 264 (1994) 413.
- [3] C. Zener, Phys. Rev. 82 (1951) 403.
- [4] A.J. Millis, P.B. Littlewood, B.I. Shraiman, Phys. Rev. Lett. 74 (1995) 5144.
- [5] H.Y. Hwang, S.-W. Cheong, N.P. Ong, B. Batlogg, Phys. Rev. Lett. 77 (1996) 2041.
- [6] X.W. Li, A. Gupta, G. Xiao, G.Q. Gong, Appl. Phys. Lett. 71 (1997) 1124.
- [7] V.V. Srinivasu, S.E. Lofland, S.M. Bhagat, K. Ghosh, S.D. Tyagi, J. Appl. Phys. 86 (1999) 1067.
- [8] S.D. Tyagi, S.E. Lofland, M. Dominguez, S.M. Bhagat, C. Kwon, M.C. Robson, R. Ramesh, T. Venkatesan, Appl. Phys. Lett. 68 (1996) 2893.
- [9] J.F. Hu, H.W. Qin, Solid State Commun. 116 (2000) 159, 2893.
- [10] J.F. Hu, H.W. Qin, J. Magn. Magn. Mater. 234 (2001) 419.
- [11] A. Rinkevich, A. Nossrov, V. Ustinov, V. Vassiliev, S. Petukhov, J. Appl. Phys. 91 (2002) 3693.
- [12] H.W. Qin, J.F. Hu, J. Chen, Y.Z. Wang, Z.X. Wang, J. Appl. Phys. 91 (2002) 10003.
- [13] M. Nadeem, M.J. Akhtar, A.Y. Khan, R. Shaheen, M.N. Haque, Chem. Phys. Lett. 366 (2002) 433.
- [14] G.M.B. Castro, A.R. Rodrigues, F.L.A. Machado, A.E.P. de Araujo, R.F. Jardim, A.K. Nigam, J. Alloys Compd. 369 (2004) 108.
- [15] G.M.B. Castro, A.R. Rodrigues, F.L.A. Machado, R.F. Jardim, J. Magn. Magn. Mater. 272–276 (2004) 1848.
- [16] B.I. Belevtsev, A.Ya. Kirichenko, N.T. Cherpak, G.V. Golubnichaya, I.G. Maximchuk, E.Yu. Belyayev, A.S. Panfilov, J. Fink-Finowicki, J. Magn. Magn. Mater. 281 (2004) 97.
- [17] J.F. Hu, H.W. Qin, H.D. Niu, L.M. Zhu, J. Chen, W.W. Xiao, Y. Pei, J. Magn. Magn. Mater. 261 (2003) 105.
- [18] M. Nadeem, M.J. Akhtar, A.Y. Khan, Solid State Commun. 134 (2005) 431.
- [19] J.F. Hu, H.W. Qin, Mater. Sci. Eng. B 100 (2003) 304.
- [20] S.K. Ghatak, B. Kaviaraj, T.K. Dey, J. Appl. Phys. 101 (2007) 023910.
- [21] P. Dutta, P. Dey, T.K. Nath, J. Appl. Phys. 102 (2007) 073906.
- [22] V.B. Naik, R. Mahendiran, Appl. Phys. Lett. 94 (2009) 142505.
- [23] S. Das, D. Dhak, M.S. Reis, V.S. Amaral, T.K. Dey, Mater. Chem. Phys. 120 (2010) 468.
- [24] S. Das, T.K. Dey, J. Nanosci. Nanotech. 10 (2010) 2944.
- [25] L.V. Panina, K. Mohri, K. Bushida, M. Noda, J. Appl. Phys. 76 (1994) 6198.
- [26] R.S. Beach, A.E. Berkowitz, Appl. Phys. Lett. 64 (1994) 3652.
- [27] J. Velázquez, M. Vázquez, D.X. Chen, A. Hemando, Phys. Rev. B 50 (1994) 16737.
- [28] M. Knobel, K.R. Pirota, J. Magn. Magn. Mater. 242–245 (2002) 33.
- [29] L.D. Landau, E.M. Lifshitz, L.P. Pitaevskii, Electrodynamics of Continuous Media, Butterworth–Heinemann, London, 1995.
- [30] D.X. Chen, J.L. Muñoz, IEEE Trans. Magn. 35 (1999) 1906.
- [31] J.F. Hu, H.W. Qin, J. Chen, R.K. Zheng, J. Appl. Phys. 91 (2002) 8912.
- [32] L.V. Panina, K. Mohri, T. Uchiyama, M. Noda, IEEE Trans. Magn. 31 (1995) 1249.
- [33] Y.F. Wang, J.F. Hu, Q.F. Huang, Y.J. Zhang, E.S. Cao, H.W. Qin, L.B. Chen, B. Li, unpublished results.